# Chiroptical Dissymmetries in Fluorescence Excitation from Single Molecules of (M-2) Helicene Dimers

Austin Cyphersmith, Sravan Surampudi, Mary J. Casey, Kathryn Jankowski, Dhandapani Venkataraman,* and Michael D. Barnes*

Department of Chemistry, and Department of Physics, University of Massachusetts—Amherst, Amherst, Massachusetts 01002, United States

S *Supporting Information*

ABSTRACT: We report on the single-molecule chiroptical properties of "right"-handed bridged triaryl amine helicene dimers, MH2. Using an experimental setup to precisely define the circular excitation polarization at the sample plane, we investigated the circular dichroic response in luminescence from individual molecules in which induced ellipticity from microscope optics is minimized. Our results comparing circular anisotropies in fluorescence excitation from MH2 and perylene diimide (PDI), an achiral, centrosymmetric chromophore, demonstrate a significant reduction in the breadth of the distribution of circular dissymmetry parameters obtained from modulation of the circularly polarized excitation source (457 nm). For PDI, we observe a symmetric distribution of circular anisotropy parameters centered about zero, with a fwhm of 0.25. For MH2, we observe an asymmetric distribution peaked at $g = -0.09$, with a slightly larger width as the corresponding PDI distribution. These results indicate that the large dissymmetry parameters ($|g| > 0.5$) in fluorescence excitation described in our original report (Hassey, R.; et al. *Chirality* **2008**, *20*, 1039−1046 and Hassey, R.; et al. *Science* **2006**, *314*, 1437−1439) were indeed affected by (at the time, unknown) linear polarization artifacts. However, the present results on MH2 provide compelling evidence for single-molecule circular dissymmetries much larger than solution or thin-film ensemble values, defined primarily by the enhanced rotatory strength (relative to the monomer), and restricted orientation at the sample surface.
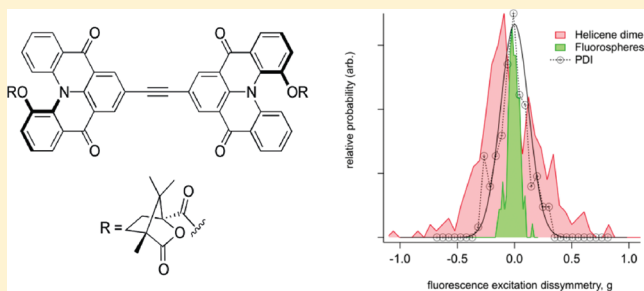
S ingle-molecule spectroscopy (SMS) emerged in the early 1990s as a uniquely powerful tool for uncovering heterogeneities in structure and local environment normally hidden under ensemble averaging.[1−3] SMS now finds applications in virtually all realms of physical science, from biotechnology to materials science and renewable energy research. However, only very recently have SMS tools been applied to exploration of hidden heterogeneities in the chiroptical response of single molecules and nanostructures.[4−6]

The fundamental question addressed in these studies is whether the typically small (~10^{-3} in absorption, for example) ensemble-averaged circular dissymmetry is *intrinsic* (i.e, is the single-molecule response representative of the average?) or *extrinsic* (is the small ensemble dissymmetry a result of extensive averaging over a range of different molecular contributions?). The relative scaling from magnetic dipole and electric quadrupole components to the rotatory strength is usually (rightfully) assumed to be orders of magnitude smaller than the normal electric dipole contributions. On the other hand, recent elegant gas-phase circular polarimetry measure-ments[7−9] and Mueller-matrix microscopy and polarimetry of crystalline materials[10−12] have demonstrated the exquisite sensitivity of molecular chiroptical response to solvation, local environment, and molecular orientation. Another interesting

exception to the small dissymmetry "rule" in molecular circular dichroism can be seen in supramolecular cholesteric chiral assemblies, where collective interactions can give rise to dissymmetries in absorption of order unity.[13,14]

In a recent article in this Journal,[15−17] Cohen called into question results presented in our published work on the dissymmetric photoluminescence intensity response of single (M/P) helicene molecules with modulated circularly polarized excitation polarization. Cohen showed how a variable retarder placed before the dichroic filter could be used to compensate for any induced linear polarization, thus presenting a precisely defined circular excitation polarization to the sample. Here, we show that Cohen's criticisms of our measurements were partially justified; however, with a similar microscope configuration as that of ref 15 (details are in the Supporting Information), we still observe a net dissymmetry in fluorescence excitation from the MH2 sample. Our results show that the distribution of dissymmetries in fluorescence excitation from the dimeric form of (M-2) helicene is indeed considerably narrower than we previously observed for the

monomeric system. However, we also show that dissymmetry factors in fluorescence excitation of order 0.1 or larger are readily observable. Comparison with fluorescence excitation dissymmetries from single molecules of perylene diimide (PDI), an achiral centrosymmetric chromophore, indicates the persistence of a small residual ellipticity even with the configurational modifications. Despite this, we are able to show a (weak) negative dissymmetric circular response in fluorescence excitation from single MH2 molecules.

Figure 1 shows a structural schematic and solution-phase circular dichroism spectra of the (M-2) helicene monomer and
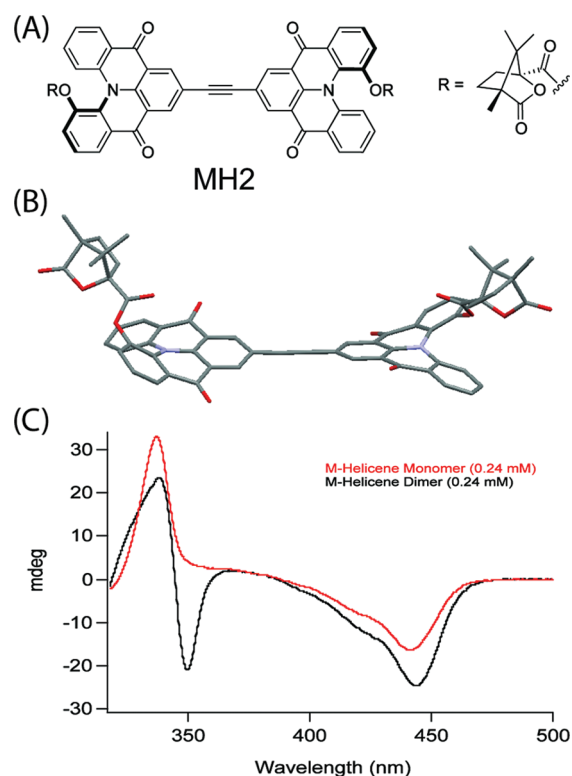

Figure 1. (A,B) Structural schematic of the M-bridged triaryl amine helicene dimer MH2. (C) Circular dichroism spectra of the M-2 monomer and dimer, each at 2.4×10^{-4} M.

the (M-2) helicene dimer, MH2.[18] The dimeric form of the "right"-handed bridged triaryl amine helicene was formed via an ethylene linkage using palladium(0)-mediated Stille coupling starting from enantiomerically pure bridged triarylamine helicene monomer.[19] Bulk circular dichroism measurements comparing the monomer and dimer indicate an approximately additive circular dichroic dissymmetry ~2× larger than the monomer at 457 nm. The structure of the helicene dimer also invites interesting questions regarding coupling of chiroptical response from monomeric segments as well as presumably restricting the range of orientations that can be presented at the surface.

Samples were drop-cast from acetonitrile solution (~10^{-10} M) onto plasma-cleaned glass coverslips. We used the 457 nm line from an air-cooled continuous wave Ar$^+$ laser as the excitation source. The excitation beam passed through a linear analyzer followed by a variable retarder, acting as a zero wave or half wave plate. A quarter wave plate was placed between the dichroic and the objective, ensuring that the circularly polarized light did not reflect off of the dichroic filter. Our tests of circular

polarization purity at the sample plane measuring extinction of the retroreflected beam indicated an ellipticity of <2%. Molecular fluorescence was detected with a high-sensitivity CCD camera (Roper Scientific Photon-Max), using a 2 s exposure time and 20 s of dwell time for each polarization half-cycle. The excitation polarization switching was synchronized with the CCD camera to alternate RCP/LCP excitation polarization (~30 ms switching time), and each single-molecule intensity trajectory was checked for accurate background subtraction.

As a control molecule, we selected PDI, a stable, achiral centrosymmetric chromophore with relatively strong absorption at 514 nm. The choice of PDI as a control chromophore was based on the idea that achiral molecules that belong to the C_{2v} or C_s point groups can exhibit apparent chiroptical effects for certain orientations.[20−23] This optical activity associated with achiral molecules derives from the fact that the projection of the magnetic dipole (oriented perpendicular to the molecular frame for π-conjugated systems) onto the electric dipole is nonzero for certain out-of-plane molecular frame orientations, giving rise to a preferential response for right or left circularly polarized excitation.[23] A small complication is the fact that the absorption cross section for PDI at 457 nm is small compared to its peak around 500 nm, thus necessitating the execution of the PDI control experiments with a different laser line than that for the MH2 system. Our diagnostics indicated that the polarization characteristics were similar for the two excitation wavelengths.

Figure 2 shows representative intensity trajectories from single molecules of PDI under alternating RCP/LCP excitation. As seen in the sample trajectory in Figure 2B, a small fraction of the PDI molecules show significant contrast ($|g| \approx 0.3$), indicating that the circular polarized excitation fields retain a small ellipticity despite the optimized retardance. In some cases, intensity fluctuations from individual molecules also contribute to breadth and uncertainty in the circular dissymmetry parameters in fluorescence excitation. This is particularly problematic for systems with strong photobleaching and fluorescence intermittency.

Figure 3 shows sample trajectories of MH2 under identical excitation intensity and (R/L-CP) polarization modulation cycles. The trajectory shown in Figure 3A appears to be fairly typical of most of the molecules surveyed, with very low contrast in photoluminescence intensity between excitation polarization cycles. We also find many examples of trajectories of the type shown in Figure 3B and C, with significant contrast in PL intensity, on the order of 0.1−0.2. The trajectory shown in Figure 3D is particularly interesting as it seems to show a fluctuating dissymmetric response possibly indicative of the two chiral chromophores acting either independently or additively. It is particularly noteworthy to point out that the signal-to-noise ratios in these (typical) measurements are considerably higher than those reported by Cohen,[15] seeming to support our conjecture that the larger dissymmetries (in fluorescence excitation) were associated with brighter, more photostable molecules. Thus, an important difference between the two sets of measurements was the way that the molecules were assayed.

Figure 4 shows a comparison of histograms of measured circular dissymmetry factors from ~250 MH2 molecules, PDI, and 20 nm dye-doped polymer nanospheres under the same experimental conditions. The dissymmetry factor, g, is defined by convention as $2(I_L − I_R)/(I_L + I_R)$, where $I_{L/R}$ are the number of detected PL counts for each polarization dwell cycle.
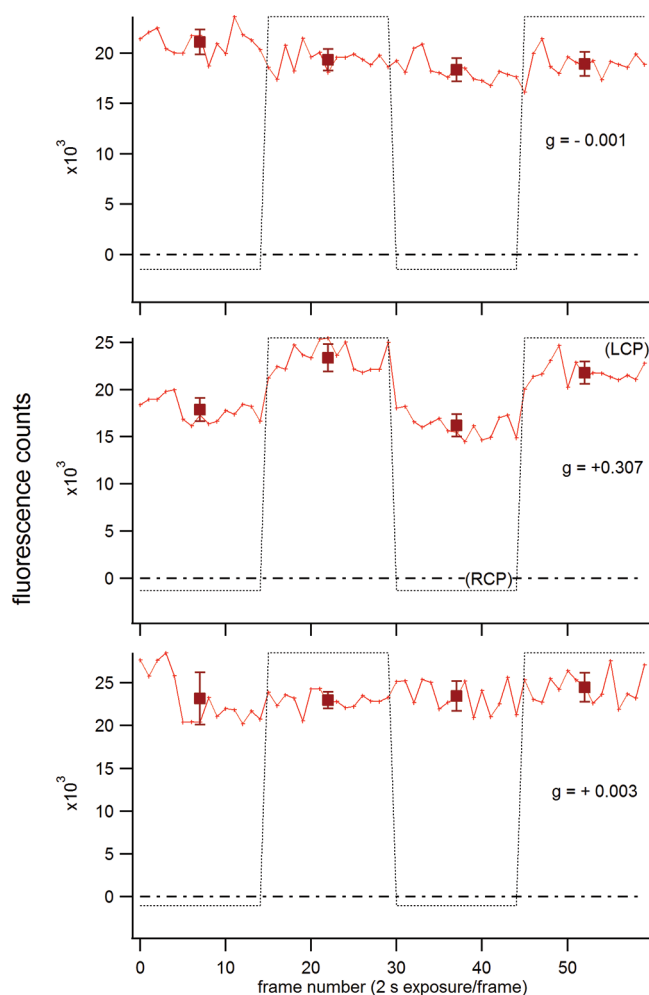
Figure 2. Sample photoluminescence intensity trajectories from single PDI molecules under alternating R/L circular polarized excitation. Dwell times for each excitation polarization were 30 s (15 × 2 s exposure/frame), and the excitation polarization state is indicated by gray dashed line (Max = LCP; Min = RCP). Solid symbols (and error bars) show mean signal levels (and standard deviations) for each polarization half-cycle. Shot-noise, intensity fluctuations and blinking, as well as small residual ellipticity (B) in the excitation field all contribute to the breadth of the circular dissymmetry distribution.

We note that the width of the nanosphere dissymmetry histogram carries information primarily on intensity variations at the sample plane under polarization modulation and is much narrower than that in our previous reports, with an average value of −0.0002 and a 2-sigma width of ±0.02. The PDI dissymmetry parameter distribution is symmetric about zero ($\langle g \rangle$ = +0.0097), whose width (fwhm = 0.26) reflects both intensity fluctuations and imperfections in the excitation field. The corresponding distribution for the MH2 sample is slightly *asymmetric*, with an average value of $\langle g \rangle$ = −0.09 (−0.12 peak) and a fwhm of 0.52, thus indicating fluorescence behavior distinct from the PDI control system.

The observation of circular dissymmetries of order ≈ 0.1 seems to suggest that, at least for the kinds of systems explored here, the small net dichroic response is a result of extrinsic factors such as the local dielectric environment. Because of the structural nature of the molecule, we assume that heterogeneity in orientation is minimal, although more work in experiment and simulation is required to verify this. In summary, it is clear
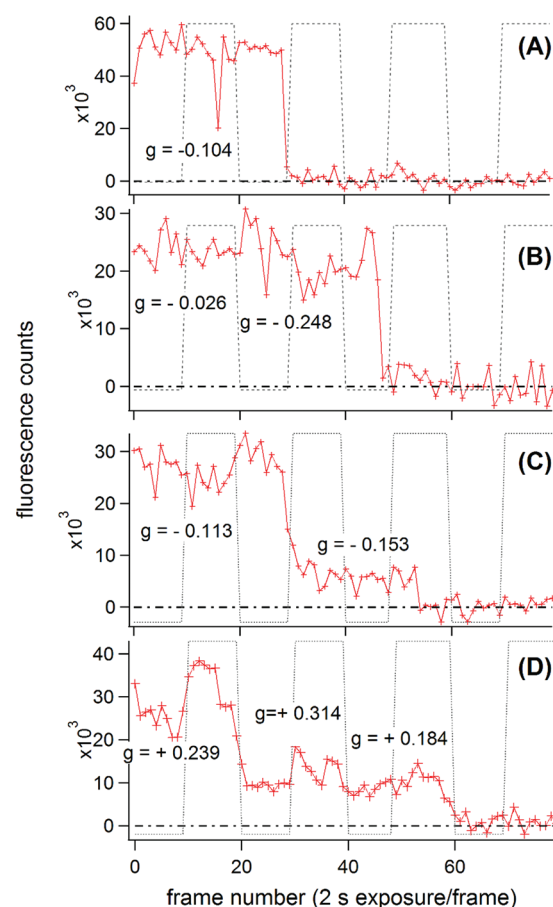

Figure 3. Sample photoluminescence intensity trajectories from single MH2 molecules under alternating R/L circular polarized excitation. Dwell times for each excitation polarization were 20 s (10 × 2 s exposure/frame). The excitation polarization state is indicated by gray dashed line (Max = LCP; Min = RCP). Examples of gross intensity switching are shown in (C) and (D).
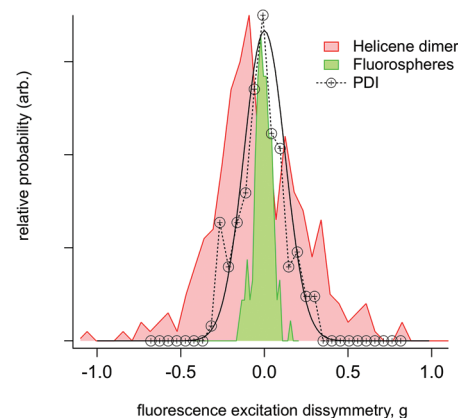

Figure 4. Histograms of the dissymmetry parameter from ∼200 single molecules of PDI (black circles) and ∼400 M-helicene dimer (red) and Yellow nanospheres (green). The dissymmetry distribution for the nanospheres is characterized by $\langle g \rangle$ = −0.0002 and a fwhm of 0.06. The MH2 distribution is peaked at g = −0.12 ($\langle g \rangle$ = −0.09), while the corresponding distribution for PDI is symmetric about g = 0 ($\langle g \rangle$ = +0.0097), with a standard deviation of 0.125.

from the present experiments that our previous measurements of circular dissymmetry in the fluorescence excitation of single helicene molecules was influenced by (at the time, unknown)

linear polarization artifacts. Even with the significant improvements in purity of circular polarization presented to the sample afforded by the generation of circularly polarized light after the dichroic, the PDI measurements indicate a weak ellipticity in the excitation field that manifests as reasonable large ($|g| > 0.3$) circular dissymmetries that average to zero. However, the present measurements on the M-helicene dimer also show that a weak net-negative circular dissymmetry is observable. The distribution of circular dissymmetry parameters for the MH2 system in the current configuration is considerably narrower than that in our previous reports on single molecules of (M/P)-helicene monomers, peaked at $g = -0.12$ (approximately 1 standard deviation from the mean of the corresponding PDI distribution). As shown by the correlation between the PL count rate and circular dissymmetry, shot-noise and intensity fluctuations also contribute to the width of the distribution and hence the resolving power of the measurement. Future experiments will be aimed at stabilization of the single-molecule PL signals and further refinement of the polarization purity of the excitation field.

■ ASSOCIATED CONTENT

Ⓢ Supporting Information

Descriptions of the experimental procedure and microscope configuration. This material is available free of charge via the Internet at http://pubs.acs.org.

■ AUTHOR INFORMATION

Notes

The authors declare no competing financial interest.

■ REFERENCES

(1) Tamarat, P.; Maali, A.; Lounis, B.; Orrit, M. *J. Phys. Chem. A* **2000**, *104*, 1−16.

(2) Dickson, R. M.; Cubitt, A. B.; Tsien, R. Y.; Moerner, W. E. *Nature* **1997**, *388*, 355−358.

(3) Moerner, W. E.; Orrit, M. *Science* **1999**, *283*, 1670−1676.

(4) Cyphersmith, A.; Maksov, A.; Hassey-Paradise, R.; McCarthy, K. D.; Barnes, M. D. *J. Phys. Chem. Lett.* **2011**, *2*, 661−665.

(5) Hassey, R.; McCarthy, K. D.; Basak, E. S. D.; Venkataraman, D.; Barnes, M. D. *Chirality* **2008**, *20*, 1039−1046.

(6) Hassey, R.; Swain, E. J.; Hammer, N. I.; Venkataraman, D.; Barnes, M. D. *Science* **2006**, *314*, 1437−1439.

(7) Muller, T.; Wiberg, K. B.; Vaccaro, P. H. *Rev. Sci. Instrum.* **2002**, *73*, 1340−1342.

(8) Muller, T.; Wiberg, K. B.; Vaccaro, P. H.; Cheeseman, J. R.; Frisch, M. J. *J. Opt. Soc. Am. B* **2002**, *19*, 125−141.

(9) Muller, T.; Wiberg, K. B.; Vaccaro, P. H. *J. Phys. Chem. A* **2000**, *104*, 5959−5968.

(10) Kahr, B.; Freudenthal, J.; Gunn, E. *Acc. Chem. Res.* **2010**, *43*, 684−692.

(11) Shtukenberg, A. G.; Freudenthal, J.; Kahr, B. *J. Am. Chem. Soc.* **2010**, *132*, 9341−9349.

(12) Arteaga, O.; Freudenthal, J.; Kahr, B. *J. Appl. Crystallogr.* **2012**, *45*, 279−291.

(13) Lakhwani, G.; Meskers, S. C. J. *J. Phys. Chem. Lett.* **2011**, *2*, 1497−1501.

(14) Savoini, M.; Biagioni, P.; Meskers, S. C. J.; Duo, L.; Hecht, B.; Finazzi, M. *J. Phys. Chem. Lett.* **2011**, *2*, 1359−1362.

(15) Tang, Y. Q.; Cook, T. A.; Cohen, A. E. *J. Phys. Chem. A* **2009**, *113*, 6213−6216.

(16) Barnes, M. D.; Paradise, R. H.; Swain, E.; Venkataraman, D.; Hammer, N. I. *J. Phys. Chem. A* **2009**, *113*, 9757−9758.

(17) Cohen, A.; Tang, Y. Q. *J. Phys. Chem. A* **2009**, *113*, 9759−9759.

(18) Surampudi, S. K.; Nagarjuna, G.; Okamoto, D.; Chaudhuri, P. D.; Venkataraman, D. *J. Org. Chem.* **2012**, *77*, 2074−2079.

(19) Field, J. E.; Hill, T. J.; Venkataraman, D. *J. Org. Chem.* **2003**, *68*, 6071−6078.

(20) Claborn, K.; Isborn, C.; Kaminsky, W.; Kahr, B. *Angew. Chem., Int. Ed.* **2008**, *47*, 5706−5717.

(21) Isborn, C. M.; Claborn, K.; Kahr, B.; Li, X. S. *Abstr. Pap. Am. Chem. Soc.* **2007**, 233.

(22) Claborn, K.; Cedres, J. H.; Isborn, C.; Zozulya, A.; Weckert, E.; Kaminsky, W.; Kahr, B. *J. Am. Chem. Soc.* **2006**, *128*, 14746−14747.

(23) Murphy, V. L.; Kahr, B. *J. Am. Chem. Soc.* **2011**, *133*, 12918−12921.